Geol. Mag. **146** (*2*), *2009, pp. 276–290. © 2008 Cambridge University Press*
doi:10.1017/S0016756808005566 *Printed in the United Kingdom*

The origin, cooling and alteration of A-type granites in southern Israel (northernmost Arabian–Nubian shield): a multi-mineral oxygen isotope study

ADAR STEINITZ*§, YARON KATZIR*, JOHN W. VALLEY‡,
YARON BE'ERI-SHLEVIN* & MICHAEL J. SPICUZZA‡

*Department of Geological and Environmental Sciences, Ben Gurion University of the Negev, Be'er Sheva 84105, Israel
‡Department of Geology and Geophysics, University of Wisconsin, Madison, WI 53706, USA

(*Received* 31 March 2008; *accepted* 16 June 2008; First published online 27 October 2008)

Abstract – A multi-mineral oxygen isotope study sheds light on the origin, cooling and alteration of Late Neoproterozoic A-type granites in the Arabian–Nubian shield of southern Israel. The oxygen isotope ratio of zircon of the Timna monzodiorite, quartz syenite and alkaline granite are within the range of mantle zircon (δ^{18}O(Zrn) = 5.3 ± 0.6 ‰, 2σ), supporting the co-genetic mantle-derived origin previously suggested based on geochemical data and similar εNd(T) values and U–Pb ages (610 Ma). Likewise, olivine norite xenoliths within the monzodiorite (δ^{18}O(Ol) = 5.41 ± 0.07 ‰) may have formed as cumulate in a parent mantle-derived magma. Within the Timna igneous complex, the latest and most evolved intrusion, an alkaline granite, has the least contaminated isotope ratio (δ^{18}O(Zrn) = 5.50 ± 0.02 ‰), whereas its inferred parental monzodiorite magma has slightly higher and more variable δ^{18}O(Zrn) values (5.60 to 5.93 ‰). The small isotope variation may be accounted for either by small differences in the temperature of zircon crystallization or by minor contamination of the parent magma followed by shallow emplacement and intrusion by the Timna alkaline granite. The Timna alkaline granite evolved, however, from a non-contaminated batch of mantle-derived magma. The formation of Yehoshafat granite (605 Ma; δ^{18}O(Zrn) = 6.63 ± 0.10 ‰), exposed ~ 30 km to the south of the mineralogically comparable Timna alkaline granite, involved significant contribution from supracrustal rocks. A-type granites in southern Israel thus formed by differentiation of mantle-derived magma and upper crustal melting coevally. Fast grain boundary diffusion modelling and measured quartz-zircon fractionations demonstrate that the Timna and Yehoshafat alkaline granites cooled very rapidly below 600 °C in accordance with being epizonal. One to three orders of magnitude slower cooling is calculated for 30 Ma older calc-alkaline granites of the host batholith, indicating a transition from thick orogenic to extended crust. Significant elevation of the δ^{18}O of feldspars occurred through water–rock interaction at moderate temperatures (100–250 °C), most probably during a thermal event in Early Carboniferous times.

Keywords: oxygen isotopes, A-type granites, Arabian–Nubian shield, Israel, zircon.

1. Introduction

The term 'A-type granites' was first coined three decades ago to define a distinct group of anorogenic granites that occur in rift zones and stable continents (Loiselle & Wones, 1979). These are usually mildly alkaline granites that crystallized under low H_2O and oxygen fugacities ('anhydrous'). In a modern non-genetic and non-tectonic granite classification scheme, A-type granites are characterized as 'ferroan, alkaline to alkali-calcic, metaluminous, slightly peraluminous, and peralkaline' (Frost *et al.* 2001). The origin of A-type granites is a long-standing geological problem. Their occurrence in intra-plate settings at a post-orogenic, cratonic stage was often related to crustal extension (e.g. Pollack, 1986; Eby, 1990; Windley, 1993; Black & Liegeois, 1993; Whalen *et al.* 1996). However, in a recent reconnaissance, Bonin (2007) stresses that although many petrogenetic models imply crustal derivation, no A-type melts were experimentally produced from crustal materials, and thus they most likely come from mantle-derived transitional to alkaline mafic to intermediate magmas. Many workers agree that the process begins with a mantle-derived melt that ascends through the lower crust and undergoes partial fractional crystallization (Stern & Gottfried, 1986; Turner, Foden & Morrison, 1992; Whalen *et al.* 1994). The rising hot magma can cause anatexis of the existing crust and possibly mix with felsic melts to create hybrid magmas (e.g. Collins *et al.* 1982; Whalen, Currie & Chappell, 1987; Creaser, Prince & Worman, 1991; Eby, 1990, 1992). Further ascent and fractionation would result in emplacement of granitoids in the upper crust. Thus, regardless of the particular mechanism for the generation of A-type granites, mantle-derived material is thought to be involved either solely as a heat source, or by providing a parent melt for evolved and hybrid magmas.

In the Arabian–Nubian shield, a Neoproterozoic juvenile crustal province that straddles both shores

§ Author for correspondence: adar.steinitz@ucalgary.ca; current address: Department of Geoscience, University of Calgary, Calgary, AB T2N 1N4, Canada.

of the Red Sea, A-type granites intruded the newly formed continental crust in the last, post-orogenic evolutionary stage at *c.* 610 to 580 Ma (Bentor, 1985; Black & Liegeois, 1993; Genna *et al.* 2002). Based on their mantle-like radiogenic isotope ratios and their ages being similar to associated alkaline mafic rocks, A-type granites in the northern Arabian–Nubian shield are thought to have formed by fractional crystallization of mafic, mantle-derived magma with little or no crustal contamination (Stern & Gottfried, 1986; Stern, Sellers & Gottfried, 1988; Beyth *et al.* 1994; Kessel, Stein & Navon, 1998; Mushkin *et al.* 2003; Jarrar *et al.* 2003). However, the petrogenetic interpretation of Nd and Sr isotope ratios in the Arabian–Nubian shield is ambiguous, since most of its crust is juvenile and relatively young (< 1 Ga: Stern, 2002), and thus by the end of the Neoproterozoic it had not yet developed the radiogenic isotope signatures characteristic of ancient continental crust. Consequently, the εNd(T) values of igneous rocks of the Arabian–Nubian shield, including the A-type granites, cover a narrow range (+3 to +5) representing either an enriched mantle or juvenile crust derived from it (Stein & Hoffmann, 1992; Stern & Kröner, 1993; Furnes *et al.* 1996; Stein & Goldstein, 1996; Stern & Abdelsalam, 1998; Stern, 2002; Mushkin *et al.* 2003). In contrast, oxygen isotopes are a sensitive tracer of upper crustal contribution to magmas, regardless of juvenility (King *et al.* 1998; Peck, King & Valley, 2000; Valley *et al.* 2005). Subduction or melting of rocks that had resided close to the earth's surface and exchanged oxygen with the hydrosphere at low temperatures would eventually elevate the δ^{18}O of mantle-derived material.

A-type granites in the northern Arabian–Nubian shield are often miarolitic, and some form central plutons within ring dyke complexes. They are thus thought to be epizonal granites (Garfunkel, 1980; Eyal & Hezkiyahu, 1980; Mushkin *et al.* 1999; Katzir *et al.* 2007*a*). Although defined as anhydrous, their distinctive pink colour suggests heavy alteration of feldspars (Matthews *et al.* 1999; Katzir *et al.* 2007*a*). Whole-rock oxygen isotope analysis of granite samples may thus yield an average mixed ratio of various minerals, each affected to a different extent by post-magmatic processes. Oxygen isotope ratios of various minerals from the same pluton will instead constrain not only the origin of the pluton, but also its cooling and late alteration.

In this study we argue for diverse origins of A-type granites from the Arabian–Nubian shield of southern Israel using zircon, the ultimate preserver of magmatic δ^{18}O values (Valley, Chiarenzelli & McLelland, 1994; Valley, 2003). Constraints on the cooling rate and hydrothermal alteration associated with the emplacement of the plutons are set by comparing the oxygen isotope ratios of quartz to that of zircon. The setting of late alteration is studied using the δ^{18}O of feldspars, which are sensitive tracers of low-temperature water–rock interaction.

2. Geological setting

The Arabian–Nubian shield was formed during the Neoproterozoic East African orogenesis (*c*. 900–550 Ma: Bentor, 1985; Stern, 1994; Genna *et al.* 2002). The orogenic cycle commenced with the formation of an anomalously thick oceanic crust, suggested to be a mantle plume head (Stein & Goldstein, 1996; Stein, 2003). Island arcs developed during the subduction of the initial oceanic lithosphere and were later accreted and sutured to form a continental crust (850–650 Ma: Stoeser & Camp, 1985). Stabilization of the continent occurred by intrusion of voluminous calc-alkaline batholiths, composed mostly of granite (650–620 Ma). A-type granite plutons formed in the last stage of the shield evolution, when a fundamental transition in tectonic style, from compressional to extensional, occurred 620–580 Ma ago (Garfunkel, 1999; Meert, 2003; Johnson & Woldehaimanot, 2003).

Southern Israel along with SW Jordan, the Sinai Peninsula and the Eastern Desert of Egypt comprise the northernmost exposures of the Arabian–Nubian shield (Fig. 1). Although basement exposures in southern Israel are relatively small, they well represent three out of the four major evolutionary stages of the Arabian–Nubian shield (Bentor, 1985). These include pelitic schists and orthogneisses of island-arc origin (820–640 Ma: Kröner, Eyal & Eyal, 1990), weakly to non-metamorphosed calc-alkaline batholithic plutons (635–625 Ma: Beyth *et al.* 1994; Katz *et al.* 1998; Eyal *et al.* 2004) and post-orogenic alkaline plutonic, dyke and volcanic rocks and conglomerates (610–595 Ma: Beyth *et al.* 1994; Kessel, Stein & Navon, 1998; Mushkin *et al.* 1999; Garfunkel, 1999; Katzir *et al.* 2006). A-type granites of the last, post-orogenic, stage occur in the Timna, Amram and Yehoshafat localities of southern Israel (Fig. 1). Rhyolitic magma of A-type characteristics also occurs as dykes, flows and ash-fall deposits throughout the Precambrian outcrops in southern Israel (Agron & Bentor, 1981; Eyal & Peltz, 1994; Kessel, Stein & Navon, 1998; Mushkin *et al.* 1999; Katzir *et al.* 2007*b*).

The Timna igneous complex, composed of alkaline plutonic rocks including olivine-norite, monzodiorite, quartz syenite and alkaline-granite, is a key exposure for studying the origin, emplacement and alteration of A-type granites (Fig. 1a). Based on geochemical, geochronological and isotope data, Beyth *et al.* (1994) argued that the Timna alkaline (A-type) granite formed by fractional crystallization from mantle-derived monzodiorite parent magma. The Timna igneous complex was thus interpreted as a 610 Ma quasi-stratified alkaline magmatic cell, which formed within a 625 Ma calc-alkaline porphyry granite crust. Stable isotope and palaeomagnetic studies suggested that the alteration of the Timna igneous complex was not related to its emplacement and Early Cambrian exhumation, but was related to Neogene fluid–rock interaction initiated by the Dead Sea Transform tectonics (Marco *et al.* 1993; Beyth *et al.* 1997; Matthews *et al.* 1999).

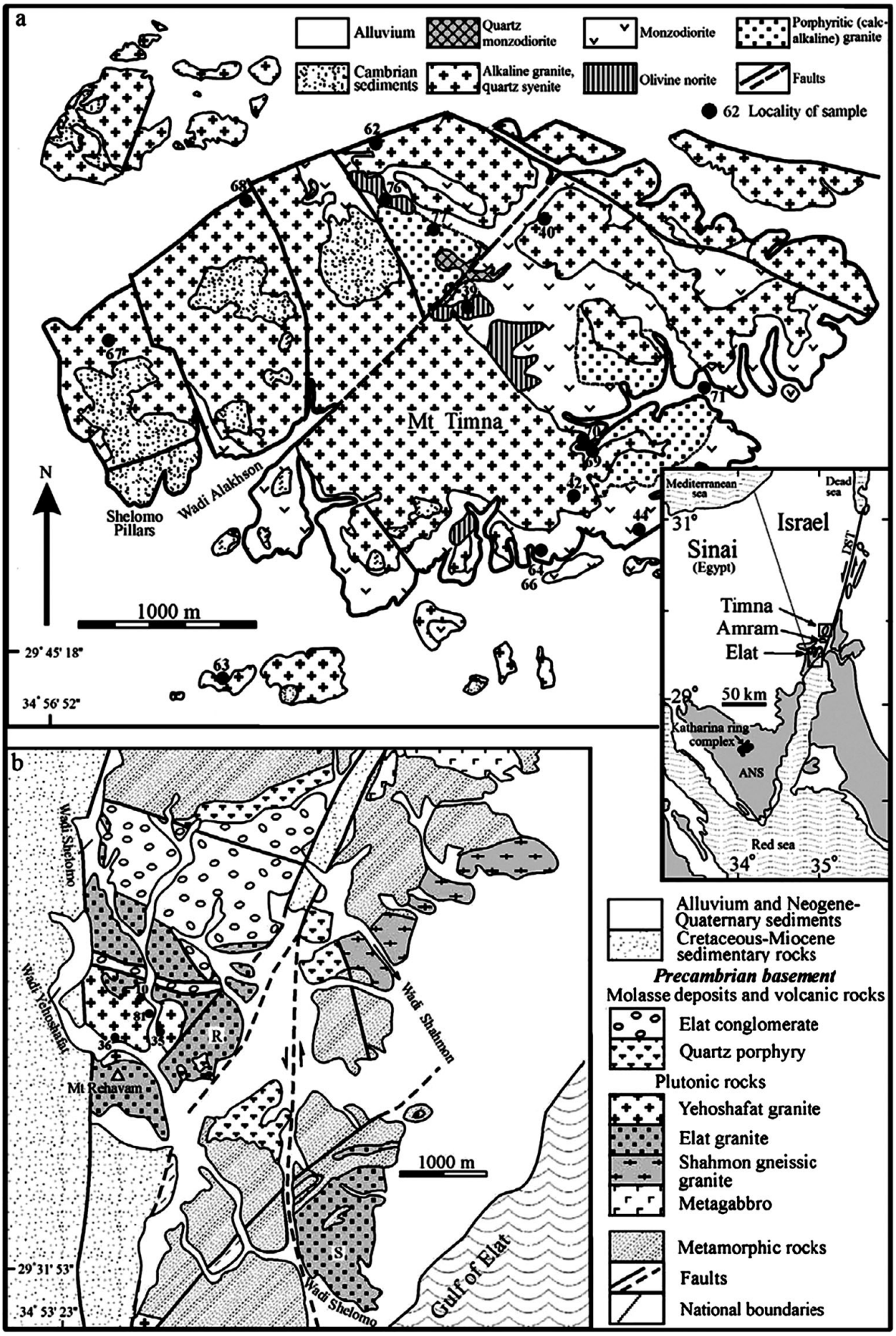

Figure 1. Simplified geological maps of the A-type granite exposures in the Arabian–Nubian shield of southern Israel. (a) The alkaline igneous complex of Timna (after Beyth *et al.* 1994). (b) The central Elat area where the Yehoshafat Granite occurs (after Eyal *et al.* 2004). R – Rehavam; S – Shelomo. Inset: a map denoting (in grey) the northernmost exposures of the Arabian–Nubian shield. DST – Dead Sea Transform.

3. Sample description

Seven plutonic rock units from southern Israel were studied in this work. Six out of seven units are of the alkaline stage and the additional pluton is the calc-alkaline Timna porphyritic granite intruded by the Timna alkaline complex. Detailed petrographic descriptions and chemical compositions of rocks and minerals are given in Shpitzer, Beyth & Matthews (1992), Beyth *et al.* (1994) and Mushkin *et al.* (2003).

The Timna porphyritic granite is composed of plagioclase (40 %), quartz (30 %), orthoclase phenocrysts ($\leq$ 2 cm; 25 %) and minor biotite. Quartz locally shows weak preferred orientation and recrystallization, implying that the Timna porphyritic granite intruded prior to the cessation of deformation in a late to post-orogenic setting. The alkaline intrusive complex in Timna includes the following lithologies: (1) Timna olivine norite is characterized by poikiloblastic texture of olivine (35 %) enclosed in orthopyroxene (5 %) and plagioclase (15 %), indicating a cumulate origin. Orthopyroxene is overgrown by brown amphibole (30 %) and biotite (15 %). The olivine norite is exposed as scattered $\leq$ 0.05 km^2-sized lenses, possibly xenoliths, engulfed by the Timna monzodiorite. (2) Timna monzodiorite varies in the modal ratios of plagioclase (45–60 %) to alkali feldspar (5–20 %) and hornblende (10–30 %) to biotite (2–20 %). (3) Timna quartz syenite consists of alkali feldspar (75 %), quartz (10 %), hornblende (7 %) and minor biotite and is rich in melanocratic rounded enclaves. In previous studies it was grouped together with the Timna alkaline granite into one mapping unit (Fig. 1a). (4) Timna alkaline granite consists of alkali-feldspar (45 %), quartz (30–40 %), plagioclase (15–25 %) and minor biotite. Timna alkaline granite is the most abundant rock in the Timna igneous complex and contains xenoliths of all previous rock units (Shpitzer, Beyth & Matthews, 1992). Yehoshafat granite is exposed in a small outcrop in the Elat block, 25 km south of Timna, and is intrusive into the peraluminous calc-alkaline Elat granite. It consists of alkali feldspar (50 %), quartz (35 %) and plagioclase (15 %). Amram quartz syenite, previously defined as alkali-granite (Mushkin *et al.* 1999), is exposed approximately half-way between Timna and the Yehoshafat granite. In addition to alkali feldspar (70 %) and quartz (20 %), it is very rich in iron oxides and hydroxides (10 %).

The alkaline granite plutons of Timna and Yehoshafat are high-K and slightly peraluminous to metaluminous (A/CNK = 0.95–1.08) and the Timna monzodiorite plots in the shoshonitic field in K_2O v. SiO_2 space. On the MALI and #Fe$*$ v. SiO_2 diagrams of Frost *et al.* (2001), the Timna and Yehoshafat alkaline granites are calc-alkalic to alkali-calcic and ferroan, respectively. The host rocks in Timna and Elat, the Timna porphyritic granite and Elat granite, respectively, are calcic to calc-alkalic and magnesian.

Zircons of the alkaline plutons and of the Timna porphyritic granite are yellowish to pink, euhedral, and generally show simple oscillatory magmatic zoning in CL images (Fig. 2). Zircon grain boundaries do not show any evidence for dissolution or resorption. Recent ion-microprobe U–Pb dating of zircons has shown that inheritance is very minor to non-existent in the studied rocks and that U–Th concentrations and ratios are magmatic (Be'eri-Shlevin, unpub. data). The oxygen isotope ratios of zircon measured in this work thus represent the magmatic values.

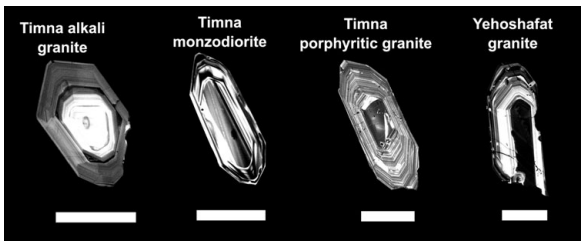

Figure 2. Cathodoluminescence images of representative zircon crystals from Timna alkaline granite, Timna monzodiorite, Timna porphyry granite and Yehoshafat granite. White bars are 100 microns. Zircons are characterized by simple magmatic oscillatory zoning and lack of dissolution at grain boundaries. Even where rim oscillatory zoning may be suspected to cut core oscillatory zoning, both core and rim gave the same age (Be'eri-Shlevin, unpub. data).

4. Analytical methods

Each unit was sampled more than once to reflect its lithological diversity. Rock samples ($\leq$ 10 kg) were crushed and sieved and mineral separates were produced by magnetic and heavy-liquid techniques. Zircon separates were cleaned by immersion in cold HNO_3 and HF to dissolve apatite and metamict zircon, respectively. Quartz separates were soaked in HF for one minute to reveal contaminant feldspar. All mineral separates were further purified by hand-picking under a binocular microscope.

Oxygen isotope analysis was performed using the laser fluorination technique at the University of Wisconsin–Madison. BrF_5 was used as the reagent. Oxygen was purified cryogenically and with an inline Hg diffusion pump, converted to CO_2 using a hot graphite rod, and analysed on a Finnigan MAT 251 mass spectrometer (Valley *et al.* 1995). Quartz separates (1.5 to 2 mg/analysis) were analysed using the rapid heating, defocused beam technique (Spicuzza *et al.* 1998). Plagioclase and K-feldspar separates, which might react appreciably with BrF_5 at room temperature, were analysed (2 to 2.5 mg/analysis) using an 'air-lock' sample chamber (Spicuzza, Valley & McConnell, 1998). Out of the overall 80 mineral separates analysed, 19 were duplicated with average reproducibility of $\pm$ 0.04 ‰ (n = 9) for zircon, $\pm$ 0.11 ‰ (n = 3) for quartz and $\pm$ 0.09 ‰ (n = 6) for titanite. During each day of analysis at least four aliquots of UW Gore Mountain Garnet standard (UWG-2) were analysed. The accepted $\delta^{18}O$ value of UWG-2 is 5.8 ‰ (Valley

Table 1. Oxygen isotope ratios of minerals from felsic to intermediate rocks of Timna and Elat, Israel

Sample	Rock	Titanite	Hornblende	Alkali feldspar	Plagioclase	Quartz	Zircon
69	Timna porphyritic granite			8.64	7.62	6.91	6.27±0.11
70				11.69	7.81	7.06	6.11±0.03
71				9.56	9.13	8.11±0.20	6.10±0.05
44	Timna monzodiorite		5.18	12.44	8.48		5.93
64		3.45	4.73	9.96	7.32		5.68±0.00
66		3.87	4.82	9.91	9.57		5.60
77		3.74	4.92	10.64	9.75		5.89±0.01
40	Timna quartz syenite	4.14	5.37	8.95	7.72		5.75
62		3.88		8.68	7.94		5.82±0.04
42	Timna alkaline granite			10.28		8.17	
63				8.52		8.50±0.11	5.52±0.03
67		4.76±0.00		8.11		8.67	5.48
68				10.35	10.03	8.40	
10	Yehoshafat granite			9.00		9.27	
35				10.35		9.22	6.52
36				11.18		9.26	6.76
81				9.85		9.13	6.60±0.04
78	Amram quartz syenite					9.00±0.11	

All values are δ^{18}O (‰, SMOW) and represent a single analysis or an average of two analyses by laser fluorination.

Table 2. Oxygen isotope ratios of minerals from mafic rocks of Timna, Israel

Rock	Sample	Orthopyroxene	Olivine	Green amphibole	Brown amphibole	Plagioclase
Timna olivine norite	39	5.78			5.26	7.21
	76		5.41±0.07	5.65	5.87	10.19

All values are δ^{18}O (‰, SMOW) and represent a single analysis or an average of two analyses by laser fluorination.

et al. 1995). The samples were analysed in two sessions, for which the overall averages of UWG-2 were 5.61 ± 0.09 ‰ and 5.56 ± 0.12 ‰. Accordingly, isotope ratios of the samples were adjusted by 0.19 ‰ and 0.24 ‰, respectively. The average value of UWG-2 during 'air lock' analysis was 5.54 ± 0.10 ‰.

5. Results

5.a. Felsic and intermediate rocks

Oxygen isotope ratios of minerals from the felsic (alkaline granite and quartz syenite) to intermediate (monzodiorite) rock units of the Timna igneous complex and of Yehoshafat granite and Amram quartz syenite are presented in Table 1 and Figure 3. Arranging the minerals in an increasing δ^{18}O order, the same general sequence is observed in all rocks: titanite, hornblende, zircon, quartz, plagioclase and alkali feldspar. This sequence is predicted by equilibrium fractionations at magmatic conditions (Valley, 2001 and references cited therein), except for the reversal between quartz and feldspars that recurs in almost all of the samples. The δ^{18}O value of alkali feldspar in the alkaline rocks from southern Israel is constantly higher than δ^{18}O(Qtz), in contrast to the observed and experimentally calibrated magmatic Δ^{18}O(Qtz–Afs) values of 1 to 1.5 ‰ (Criss & Taylor, 1983; Clayton, Goldsmith & Mayeda, 1989). This indicates that the δ^{18}O of alkali feldspar was elevated by post-magmatic alteration.

Zircon (Zrn) from the alkaline plutons of Timna (alkaline granite, monzodiorite and quartz syenite) shows a relatively narrow range of mantle-like δ^{18}O: ~ 5.5 to 5.9 ‰, while the calc-alkaline porphyritic granite of Timna has a higher δ^{18}O(Zrn) of 6.1 to 6.3 ‰ (Fig. 3). The highest δ^{18}O(Zrn) was measured in the alkaline Yehoshafat Granite: 6.52–6.76 ‰. Zircon was shown to retain its original magmatic δ^{18}O value through processes of diffusion, alteration and high-temperature metamorphism (Valley *et al.* 1994; Page *et al.* 2007). Likewise the composition of the magma (that is, SiO_2 content) and the temperature of crystallization of zircon negligibly affect the δ^{18}O value of zircon (Valley *et al.* 2005; see also Sections 6.a.1 and 6.a.2). Thus the ~ 1 ‰ difference in measured δ^{18}O(Zrn) between the Timna and Yehoshafat alkaline granites should reflect the variable contribution of mantle-derived and crustal sources to the granite magmas. In contrast to the narrow (~ 1 ‰) range in δ^{18}O(Zrn), oxygen isotope ratios of quartz measured in this study lie between 6.91 and 9.27 ‰. The range in δ^{18}O(Qtz) for the Timna alkaline granite, Timna porphyritic granite and Yehoshafat granite is 8.17–8.67 ‰ (n = 4), 6.91–8.11 ‰ (n = 3) and 9.13–9.27 ‰ (n = 4), respectively (Fig. 3). The δ^{18}O(Qtz) values measured in the Timna alkaline granite and the Timna porphyritic granite in a previous study (Beyth *et al.* 1997; one sample per pluton), 8.5 and 7.6 ‰, respectively, are within the above ranges. The measured quartz-zircon fractionations in the Timna alkaline granite and Yehoshafat granite, ~ 3 and 2.6 ‰, respectively, are higher than the equilibrium

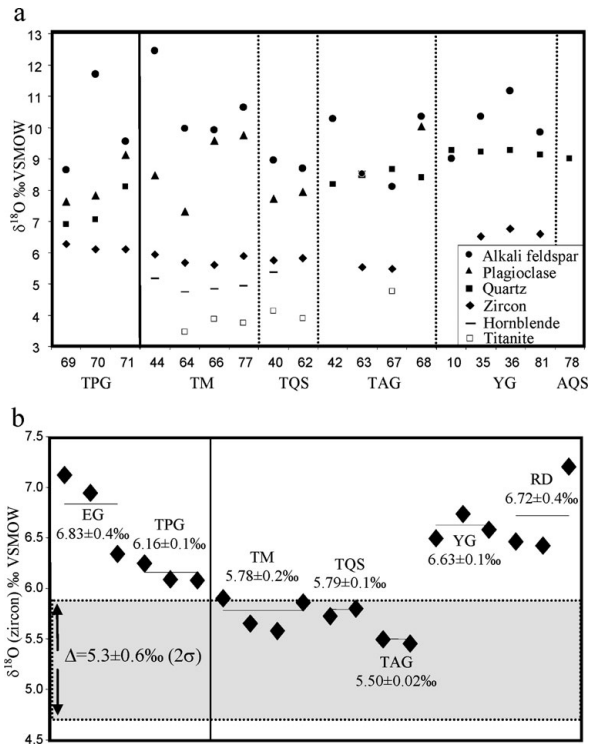

Figure 3. (a) δ^{18}O values of minerals from the A-type granites and associated rocks of southern Israel. Numbers along the horizontal axis correspond to the sample number in Table 1 and Figure 1. Vertical dashed lines separate alkaline rock units; full line separates the calc-alkalines from the alkaline rocks. (b) Enlarged view of oxygen isotope ratios of zircon (δ^{18}O(Zrn)). Horizontal lines represent the average value for each rock unit. Dashed grey rectangle shows the δ^{18}O of mantle zircon (5.3 ± 0.6 ‰, 2σ: Valley *et al.* 1998). Isotope ratios of zircon from Elat granite (EG) and alkaline rhyolite dykes (RD) of the Elat area are from Eyal *et al.* (2004) and Katzir *et al.* (2007*b*), respectively. EG – Elat Granite, TPG – Timna Porphyritic Granite, TM – Timna Monzodiorite, TQS – Timna Quartz Syenite, TAG – Timna Alkaline Granite, YG – Yehoshafat Granite, AQS – Amram Quartz Syenite, RD – Alkaline rhyolite dykes.

Δ^{18}O(Qtz–Zrn) = 2.29 at 800 °C (Valley, Bindeman & Peck, 2003). In the Timna porphyry granite, however, δ^{18}O(Qtz) values exceed δ^{18}O(Zrn) by 0.64 to 2 ‰.

If equilibrated at magmatic temperatures, hornblende and zircon should have similar δ^{18}O values (Kohn & Valley, 1998; Valley, Bindeman & Peck, 2003). However, δ^{18}O(Hbl) in the Timna monzodiorite is 0.75 to 0.95 ‰ lower than δ^{18}O(Zrn), possibly due to reset of δ^{18}O(Hbl) by subsolidus exchange with feldspars and quartz. Magmatic fractionation values between zircon and titanite, Δ^{18}O(Zrn–Ttn) = 1.2 ± 0.3 ‰ (King *et al.* 2001), were retained only in one sample of the Timna quartz syenite ($\Delta = 1.32$ ‰). Another sample of quartz syenite and all three samples of the monzodiorite show higher Δ^{18}O(Zrn–Ttn) values of 1.61 to 2.03 ‰. Lowering of δ^{18}O(Ttn) may have occurred by recrystallization of secondary hydrothermal titanite, as suggested by core-to-rim colour zoning observed in thin-sections of the monzodiorite.

5.b. Mafic rocks

Oxygen isotope ratios of minerals separated from the Timna olivine norite are given in Table 2. Fresh olivine and orthopyroxene were laboriously separated from samples AG-76 and AG-39, respectively, and yielded δ^{18}O(Ol) = 5.41 ± 0.07 ‰ and δ^{18}O(Opx) = 5.78 ‰. These values are within the range of mantle olivine, 5.18 ± 0.28 ‰, and orthopyroxene, 5.69 ± 0.28 ‰ (1σ; Mattey, Lowry & Macpherson, 1994). Likewise δ^{18}O values of brown amphibole separated from AG-39, 5.26 ‰, are similar to amphibole of numerous spinel peridotite xenoliths, 5.36 ± 0.30 ‰ (Mattey *et al.* 1994). Moreover, the Δ^{18}O(Opx-Amph) = 0.52 ‰ in AG-39 is indicative of mantle equilibration temperatures. All the above isotope evidence strongly favours a mantle origin for the olivine norite parent magma. The relatively higher δ^{18}O values of brown and green amphibole separated from AG-76 (5.65 and 5.87 ‰) are, however, indicative of hydrothermal origin.

6. Discussion

6.a. Origin of magma

6.a.1. Timna igneous complex

Within the post-orogenic alkaline plutonism of the northern Arabian–Nubian shield, the Timna igneous complex is unique: it includes intrusive rocks that vary in composition from mafic (Timna olivine norite) through intermediate (Timna monzodiorite) to felsic (Timna alkaline granite, Timna quartz syenite). Field relations within the Timna igneous complex are, however, intricate and ambiguous (Shpitzer, Beyth & Matthews, 1992). Based on geochronological, geochemical and radiogenic isotope data, Beyth *et al.* (1994) worked out the evolution of the Timna igneous complex. They concluded that: (1) the alkaline plutonic rocks of Timna are coeval (610 ± 10 Ma) and co-genetic and evolved from parental mantle-derived monzodiorite magma. Fractional crystallization within the magma chamber involved deposition of cumulate olivine norite later brought upwards as xenoliths by a new pulse of monzodiorite magma. Further differentiation ended with the formation of highly evolved alkaline granite (Timna alkaline granite), which is intrusive into the Timna monzodiorite. (2) The Timna porphyry granite shows a different geochemical affinity compared to the other plutonic rocks in Timna. It is appreciably depleted in K_2O and Rb, enriched in Sr, and has a positive Eu anomaly. Its U–Pb single zircon evaporation age (625 ± 5 Ma) is 15 Ma older than that of the alkaline rocks. It is thus part of the late to post-collisional calc-alkaline batholith of the northern Arabian–Nubian shield and represents remnants of the country rocks intruded by the alkaline series. (3) The crystalline exposure in Timna represents a Timna porphyritic granite-hosted stratified alkaline magma chamber that was first denuded during deep Late

Precambrian erosion and later faulted and exposed by Neogene tectonism related to the Dead Sea Transform.

The $\delta^{18}O$ values of olivine and orthopyroxene in the Timna olivine norite, 5.41 ± 0.07 ‰ and 5.78 ‰, respectively, are similar to those measured in mantle peridotites (1σ; Mattey, Lowry & Macpherson, 1994). Likewise the average $\delta^{18}O$(Zrn) of the Timna monzodiorite, quartz syenite and alkaline granite, 5.78 ± 0.16 ‰, 5.79 ± 0.05 ‰ and 5.50 ± 0.02 ‰, respectively, are within two standard deviations of the average $\delta^{18}O$ of mantle zircon (5.3 ± 0.6 ‰; Valley, 2003). Oxygen isotope ratios of zircon measured in the Timna alkaline plutons are thus generally compatible with origin by fractional crystallization of mantle-derived magma (Fig. 3). Fractional crystallization alone cannot explain, however, why the latest and most evolved magma in Timna, the Timna alkaline granite, has slightly lower $\delta^{18}O$(Zrn) relative to its inferred parent monzodiorite magma. Fractional crystallization can result in higher whole rock (WR) $\delta^{18}O$ values by up to ~ 1 ‰ in more silicic magmas. However, the value of $\delta^{18}O$(Zrn) remains approximately constant because the fractionation, $\Delta^{18}O$(WR-Zrn), increases at nearly the same rate as $\delta^{18}O$(WR) due to the greater proportion of high-$^{18}O/^{16}O$ minerals, quartz and feldspar, in the evolving, more silicic magmas (Valley *et al.* 2005).

The ≤ 0.3 ‰ difference in $\delta^{18}O$(Zrn) between the Timna alkaline granite and Timna monzodiorite may be the result of small differences in the temperature of zircon crystallization. If the granitic magma had crystallized zircon at a lower temperature relative to the monzodioritic magma, fractionation would have increased beyond the compositional effect, resulting in lower $\delta^{18}O$(Zrn) in the Timna alkaline granite. In order to test this premise, zircon saturation temperatures were calculated for the Timna alkaline granite and Timna monzodiorite magmas using the calibration of Watson & Harrison (1983) and the geochemical data for Timna rocks from Beyth *et al.* (1994). The average zircon saturation temperature of the Timna alkaline granite is 773 ± 3 °C (1σ; $n = 4$), whereas those calculated for the Timna monzodiorite are lower and more variable, ranging from 665 to 731 °C with an average temperature of 686 ± 33 °C ($n = 4$). Apparently, the Timna monzodiorite magma should not have crystallized zircon at all, which stands in contrast to the abundance, idiomorphism and magmatic texture of the Timna monzodiorite zircons (Fig. 2). The M cation ratios ((Na+K+2Ca)/(AlSi)) calculated for the Timna monzodiorite, 2.3 to 3.2, fall, however, far outside of the calibration range of Watson & Harrison (1983) experiments ($M = 0.9$ to 1.7). Consequently the melt structure of the Timna monzodiorite is not gauged correctly and the calculated apparent saturation temperatures may have no geological relevance (Hanchar & Watson, 2003). Likewise, other studies that attempted to extrapolate beyond the original experimental calibration, even only up to $M = 2.1$, failed to predict the abundance and textures of zircon in tonalites (Hansmann & Oberli, 1991; Von Blankenburg, 1992). The temperature at which the Timna monzodiorite magma began crystallizing zircon cannot be constrained. Thus the slightly higher $\delta^{18}O$(Zrn) values of the Timna monzodiorite and Timna quartz syenite relative to the Timna alkaline granite may represent the effect of variable zircon crystallization temperature, but may also be due to variable contributions of supracrustal material to magmas.

The relatively large range in chemical (52–56 wt % SiO_2: Beyth *et al.* 1994) and modal composition and in $\delta^{18}O$(Zrn) of the Timna monzodiorite (5.60 to 5.93 ‰) implies admixture of the monzodiorite magma with a crustal component shortly before crystallization, impeding full homogenization. Following this scenario, the Timna alkaline granite, which has uniform mantle-like isotope ratios, $\delta^{18}O(Zrn) = 5.50 \pm 0.02$ ‰, could not have evolved directly from the variably contaminated Timna monzodiorite, but from a different, purely mantle-derived, batch of magma. The parental magma of the Timna alkaline granite could be equivalent in composition to the Timna monzodiorite prior to contamination, but could also be of other mafic compositions, for example, an alkaline basalt magma that might also be the source of olivine norite cumulates. The new oxygen isotope data do not favour one of these scenarios over the other; however, the view of the Timna complex as an exposed compositionally stratified magma chamber with simple genetic relations between its components should be re-evaluated because of other considerations. First, the very large mafic magma body required to form the alkaline granite by crystal fractionation has not been identified in Timna (Beyth *et al.* 1994). Secondly, the Timna alkaline granite crystallized at shallow depth, as indicated by its miarolitic character. However, the high degree of fractional crystallization required to form residual voluminous granite melt cannot be accomplished in a shallow, rapidly cooling and crystallizing mafic magma chamber.

Based on previous (Shpitzer, Beyth & Matthews, 1992; Beyth *et al.* 1994) and our own observations and the new oxygen isotope data, a modified model for the evolution of the Timna alkaline complex is devised and schematically illustrated in Figure 4. We hypothesize that the alkaline complex of Timna is not a static magma chamber, but represents evolution at different depths within the crust. Evidence for complex intrusive relationships between mafic, intermediate and felsic bodies not only at the surface, but also at depth, is given by gravity and magnetic studies of the Timna area (Segev, Goldshmidt & Rybakov, 1999).

A mantle-derived monzodiorite magma (with a hypothetical composition of $\delta^{18}O(Zrn) = 5.5$ ‰) ponded at the middle crust (Fig. 4a). Fractional crystallization of olivine, orthopyroxene and plagioclase formed a cumulate olivine norite. While fractionating in the mid-crust, the magma assimilated the country rock at the roof of the chamber and mixed with it (Fig. 4a). Contamination caused slight and unevenly distributed

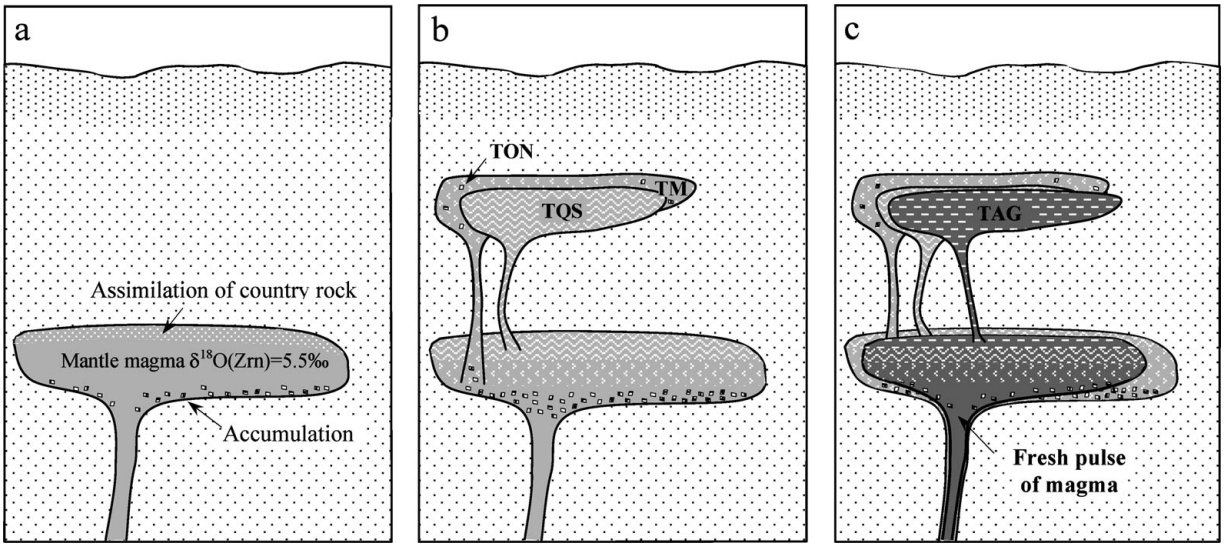

Figure 4. Evolution of the alkaline igneous complex of Timna, southern Israel, based on interpretation of field, petrographic and oxygen isotope data. (a) Mantle-derived parent monzodiorite magma ponded at mid-crustal levels. Mafic cumulates formed by fractional crystallization and sank to the bottom of the chamber. Assimilation of country rock at the roof resulted in minor elevation of δ^{18}O. (b) Fractional crystallization in the chamber formed compositional layering. A magma batch of contaminated and partially homogenized monzodiorite (TM) was emplaced at shallow levels shortly followed by magma of quartz syenite composition (TQS) that mingled with it. Xenoliths of mafic cumulates (TON) were entrained in the rising monzodiorite magma and reacted with it. (c) Replenishment of the magma chamber by a fresh batch of mantle-derived magma did not involve assimilation of country rocks due to armouring by previously deposited cumulates. Fractional crystallization resulted in generation of alkaline granite (TAG) with mantle δ^{18}O values.

elevation in the oxygen isotope ratio of the magma, manifested in the δ^{18}O(Zrn) = 5.6 to 5.9 ‰ values of the Timna monzodiorite. For example, material balance requires up to 5 % mixing with a country rock of sedimentary origin, like the abundant Elat schist (δ^{18}O(WR) = 12 ‰; Eyal *et al.* 2004), to account for the observed elevation in δ^{18}O. The contaminated monzodiorite magma (Fig. 4b) fractionated to form quartz syenite magma and was then injected upwards to form a small pluton. It carried with it xenoliths of Timna olivine norite that reacted with the evolved magma, resulting in amphibole overgrowth over orthopyroxene and olivine. A quartz syenite pluton (Fig. 4b) intruded shortly after, prior to final solidification of the monzodiorite, giving rise to magma mingling manifested in numerous mafic microgranular enclaves.

Replenishment of the chamber with a fresh batch of monzodiorite magma (Fig. 4c) was followed by differentiation to alkaline granite (Timna alkaline granite). Assimilation was inhibited by armouring of the magma chamber with previously crystallized cumulates. The Timna alkaline granite intruded last and crystallized and cooled at a shallow depth as shown by the miarolitic cavities. It preserves the non-contaminated, mantle-like δ^{18}O of the parental mafic magma.

6.a.2. Yehoshafat granite

Yehoshafat granite, a small alkaline granite pluton in the Elat area, is intrusive into the calc-alkaline Elat granite. Recent U/Pb ion microprobe dating of zircon separated from the Yehoshafat granite yielded an age of 605 ± 4 Ma (Katzir *et al.* 2006). Resemblance in petrographic and geochemical characteristics, field relations and age calls for a common origin for the Timna and Yehoshafat alkaline-granites. Surprisingly, the Yehoshafat granite has an average δ^{18}O(Zrn) of 6.63 ± 0.10 ‰ (n = 3), which is ∼ 1 ‰ higher than the mantle-like value of the Timna alkaline granite. An equally high average δ^{18}O(Zrn), 6.72 ‰, characterizes rhyolite dykes of alkaline affinity that cross-cut the Yehoshafat granite (Katzir *et al.* 2007*b*). The zircon saturation temperatures of the Timna alkaline granite and Yehoshafat granite are similar (773 °C). Thus the significant magmatic ^{18}O/^{16}O-enrichment in the Yehoshafat granite and the rhyolite dykes relative to the mantle-like Timna alkaline granite requires a considerable contribution of supracrustal rocks. Since the temperature of alkaline granite magma and its viscosity allow only negligible melting of country rocks, assimilation at the level of magma emplacement is not likely. Therefore, the ^{18}O/^{16}O enrichment of the Yehoshafat granite had to originate at depth and to involve melting of surface-derived source rocks.

The pronounced negative Eu anomaly of the Yehoshafat granite implies that it evolved (like the Timna alkaline granite) by fractional crystallization of plagioclase from a more mafic magma. However, mafic alkaline rocks of Yehoshafat granite age that may represent such parental magma are not exposed in the Elat block. Unlike the Timna alkaline granite, the Yehoshafat granite has more Na than K and it plots at the edge of the A-type field, close to the boundary

with S- and I-type granites in classification diagrams of Whalen, Currie & Chappell (1987). Thus, assuming that the Yehoshafat granite evolved from alkaline mantle-derived mafic magma requires a contribution from another high $\delta^{18}O$, non A-type source. Such sources can be potentially represented by metamorphic rocks widely exposed in the Elat block. These include the pelitic–psammitic Elat schist ($\delta^{18}O(Qtz) \approx 13$ ‰), Taba tonalitic gneiss ($\delta^{18}O(Zrn) \approx 8$ ‰) and Elat granitic gneiss ($\delta^{18}O(Zrn) \approx 7$ ‰). Whereas ~ 1 ‰ elevation in the $\delta^{18}O$ of the Yehoshafat magma by melting of orthogneisses would require unreasonably high magma/assimilant ratios, melting and mixing of Elat schist at a 3:1 ratio could explain the observed elevation in the isotope ratio. However, melting of pelites would also involve significant Al-enrichment in the magma, but the aluminium saturation indices of the Yehoshafat granite and the mantle-derived Timna alkaline granite are similar (1.02). Since no single exposed source can account for the $^{18}O/^{16}O$-enrichment, a plausible scenario would be melting and mixing of variable supracrustal rocks, followed by fractional crystallization that would eventually result in granitic magma in equilibrium with zircon of $\delta^{18}O(Zrn) = 6.6$ ‰.

In conclusion, oxygen isotope ratios of zircon show that in the northern Arabian–Nubian shield, A-type granites formed coevally from both mantle and crustal sources. Whereas the Timna alkaline granite evolved from mantle-derived magma, significant crustal melting is deduced for the Yehoshafat granite.

6.a.3. Timna porphyritic granite

The Timna porphyritic granite represents the calc-alkaline crust into which the Timna alkaline complex intruded (Beyth *et al.* 1994). The average $\delta^{18}O(Zrn)$ of the Timna porphyritic granite, 6.16 ± 0.10 ‰, is higher compared to that of the Timna alkaline series ($\delta^{18}O(Zrn)$ 5.5 to 5.9 ‰). The limited contribution of upper crustal sources indicated by the oxygen isotope ratios is compatible with the I-type character of the Timna porphyritic granite (Beyth *et al.* 1994). Its magma sources, located in the middle or lower crust, are thus different from those of the calc-alkaline peraluminous, S-type Elat granite of rather similar age, which has average $\delta^{18}O(Zrn) = 6.8$ ‰ (Eyal *et al.* 2004). Thus in two crustal blocks located only 30 km apart, the petrogenesis of both post-collision calc-alkaline and within-plate alkaline granites is fundamentally different. The E–W-trending Themed Fault, belonging to the Tertiary central Sinai-Negev shear zone, separates the Elat igneous exposures from the Timna ones. Based on geological and geophysical evidence, the Themed fault was shown to be a rejuvenated Proterozoic fault that separates the Elat block of mostly felsic basement from a northerly block of intermediate to mafic basement mostly covered by a thick Phanerozoic sedimentary sequence (Z. Garfunkel, unpub. Ph.D. thesis, Hebrew Univ. Jerusalem, 1970; Segev, Goldshmidt & Rybakov, 1999). The isotope data reiterate the spatial heterogeneity in the structure and composition of the Proterozoic basement over small distances in southern Israel.

6.b. Cooling rates of plutons

Post-crystallization closed-system diffusional exchange in slowly cooled plutonic rocks often resets the oxygen isotope ratios of many minerals. Consequently, the measured isotope fractionations between most coexisting minerals in a slowly cooled plutonic rock sample are rarely indicative of its crystallization temperature. However, the fractionation between a refractory mineral (e.g. zircon) and a mineral that exchanges oxygen more readily (e.g. quartz) may constrain the subsolidus cooling rate of a pluton. Whereas in zircon, oxygen diffusion practically ceases at ~ 800 °C (Valley, Chiarenzelli & McLelland, 1994; Page *et al.* 2007), quartz keeps on exchanging oxygen with other minerals down to subsolidus temperatures of ~ 600 °C, depending on the crystal size and cooling rate of the rock (King *et al.* 1998; Valley, 2001). Thus the deviation of the measured $\Delta^{18}O(Qtz–Zrn)$ from its expected equilibrium value at the final crystallization of granite (2.29 ‰ at 800 °C; Valley, Bindeman & Peck, 2003) may be used to evaluate cooling rates. The Fast Grain Boundary (FGB) model (Eiler, Baumgartner & Valley, 1992) considers mineral-inherent parameters (diffusion and fractionation coefficients) and rock-specific grain characteristics (grain size and shape, modal abundance) of all minerals in a rock for closed-system interdiffusion calculation (Appendix Table 1, available as supplementary material online at http://www.cambridge.org/journals/geo). Using the FGB program (Eiler, Baumgartner & Valley, 1994) we calculated the quartz-zircon oxygen isotope fractionations expected at variable cooling rates of granites in southern Israel (Fig. 5). By comparing the calculated and measured fractionations, the Precambrian cooling rates of alkaline (Fig. 5a) and calc-alkaline (Fig. 5b) plutons were constrained.

In all rock units except the Timna porphyritic granite, $\Delta^{18}O(Qtz–Zrn)$ values exceed the equilibrium fractionation at 800 °C, denoted by a dashed line in Figure 5 (2.29 ‰; Valley, Bindeman & Peck, 2003). This is indicative of retrograde oxygen exchange, whereby the further and higher from the 800 °C isotherm a rock plots, the slower it cooled below the closure temperature of quartz. Since rocks differ by their mineralogy and texture, iso-cooling-rate lines were calculated for each rock unit separately. Samples of both alkaline granites, Timna alkaline granite and Yehoshafat granite, plot close to their respective calculated 1000 °C/Ma lines (Fig. 5a). Actually, the granite plutons cooled as fast as late Precambrian alkaline rhyolite dykes in Elat, as indicated by their comparable quartz-zircon fractionations (Fig. 5a; Katzir *et al.* 2007*b*). Rapid temperature lowering to 600 °C requires either efficient heat removal by convecting fluids or

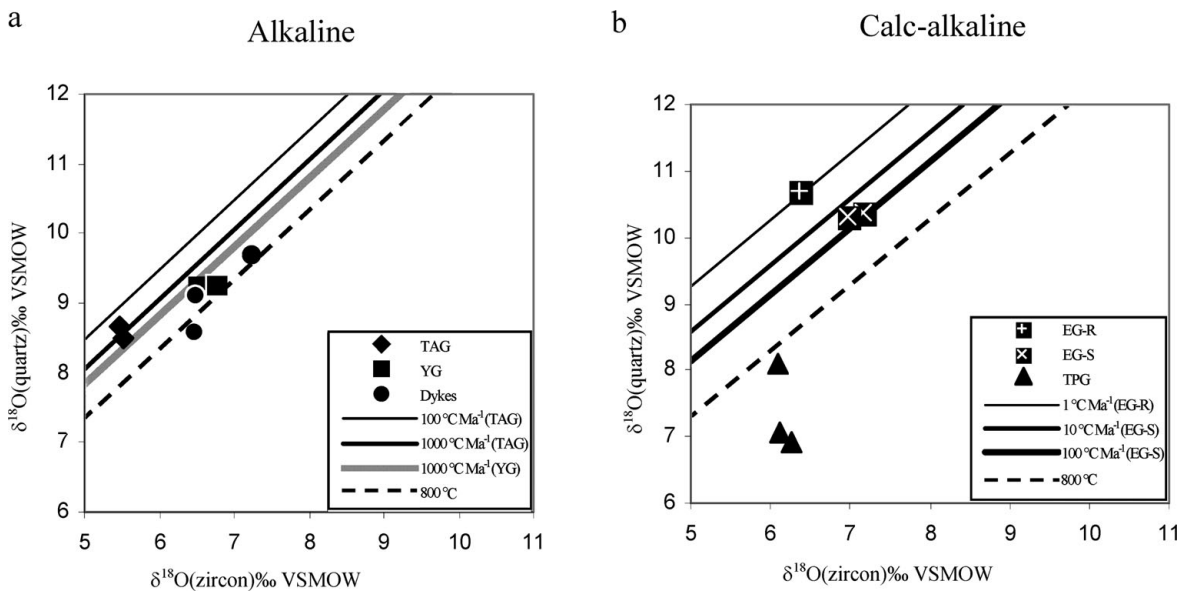

Figure 5. δ–δ diagrams for zircon and quartz in granitoid rocks from southern Israel. Iso-cooling-rate lines are calculated for each pluton based on a fast grain boundary diffusion model (see Supplementary Material). Dashed line represents equilibrium fractionation at 800 °C (Valley, Bindeman & Peck, 2003). (a) Alkaline granites from Timna (TAG) and Elat (YG) and alkaline rhyolite dykes from Elat (Katzir *et al.* 2007*b*). (b) Calc-alkaline granites including the Timna Porphyry Granite (TPG) and the Rehavam (EG-R) and Shelomo plutons (EG-S) of Elat granite (Eyal *et al.* 2004).

dry conductive cooling at very shallow crustal levels. Elevated δ^{18}O values of both quartz and feldspar in the alkaline granites rule out high-temperature fluid–rock interaction. In contrast, evidence for shallow emplacement is plentiful: both granites are fluorite-bearing and the Timna alkaline granite is particularly rich in miarolitic cavities.

An entirely different thermal history is characteristic of the former calc-alkaline granites (Fig. 5b). The δ^{18}O(Qtz) of the Timna porphyritic granite samples is scattered, and the values plot below the 800 °C isotherm. This suggests subsolidus lowering of δ^{18}O(Qtz) by interaction with heated low-δ^{18}O fluids. Textural observations suggest that hydrothermal alteration of the Timna porphyritic granite involved deformation and recrystallization of quartz. An undisturbed cooling history is, however, presented by the calc-alkaline Elat granite plutons (Eyal *et al.* 2004). Quartz-zircon fractionations in the Rehavam pluton and Shelomo pluton correspond to cooling rates of $\sim 1^{\circ}$/Ma and $< 100^{\circ}$/Ma, respectively. Rehavam pluton, the host rock of Yehoshafat granite, is more deeply eroded than Shelomo pluton (Eyal *et al.* 2004), thus explaining the difference in cooling rates calculated for the two plutons. None the less, both plutons cooled at least an order of magnitude slower than the alkaline plutons. This calls for much deeper emplacement of the Elat granite (10–15 km: Garfunkel, 1980), also indicated by its subsolvus nature and the lack of contact aureole within the meta-sedimentary country rocks (Eyal *et al.* 2004).

In situ U–Pb zircon geochronology yielded ages of 635 and 605 Ma for the Elat and Yehoshafat granites, respectively (Katzir *et al.* 2006). Thus within 30 Ma the cooling rate of plutons in southern Israel accelerated from 1–100° to $\sim$ 1000°/Ma. This indicates a fundamental change in tectonic setting from post-collisional over-thickened orogenic crust to normal or thinned cratonic crust. Whereas calc-alkaline magmas ponded at mid-crustal levels due to buoyancy, the ascent of alkaline magmas to shallow levels was assisted by extension, as also indicated by extensive injection of dyke swarms. The intrusion of the epizonal Yehoshafat granite into the mesozonal Rehavam pluton implies nearly 10 km of uplift over a period of 30 Ma. This uplift may be accommodated by moderate erosion rates (3 mm per year). Shortly after the intrusion of the Yehoshafat granite, however, major uplift, erosion and differentiation of the area to basins and highs occurred, giving rise to the deposition of the Elat conglomerate (Garfunkel, 1999).

6.c. Post-magmatic alteration

An FGB model calculation predicts that subsolidus closed-system exchange with quartz during cooling would have resulted in lowering the magmatic δ^{18}O values of alkali-feldspar in the Timna plutons and Yehoshafat granite to 6–7 ‰. However, measured δ^{18}O(Afs) values in these plutons are much higher, ranging from 8.1 to 12.4 ‰ (Fig. 3; Table 1). Measured Δ^{18}O(Qtz–Afs) values in southern Israel plutons are reversed and range from +0.5 to −4 ‰ (Fig. 6). These differ markedly from both equilibrium magmatic fractionations (Δ^{18}O(Qtz-Afs) = 0.8 at 800 °C: Clayton, Goldsmith & Mayeda, 1989) and observed fractionations in granitoids that cooled in dry conditions (0.8 to 2.0 ‰: Criss & Taylor, 1983, 1986; King & Valley, 2001). Thus isotope ratios and fractionations of alkali-feldspar cannot

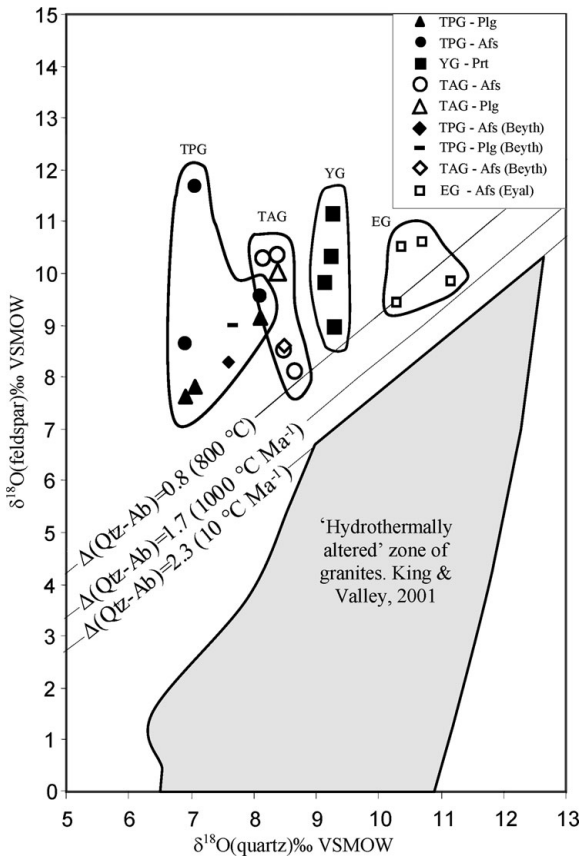

Figure 6. δ–δ diagram for quartz and feldspar (plagioclase – Plg, alkali-feldspar – Afs, perthite – Prt) in granitoid rocks of southern Israel. Beyth = Beyth *et al.* 1994; Eyal = Eyal *et al.* 2004. Lines represent equilibrium fractionation at 800 °C (Clayton, Goldsmith & Mayeda, 1989) and fractionations predicted by the FGB model calculation, for variable cooling rates. Grey area represents the range of values found in hydrothermal altered granites of the Idaho Batholith (Criss & Taylor, 1983; King & Valley, 2001).

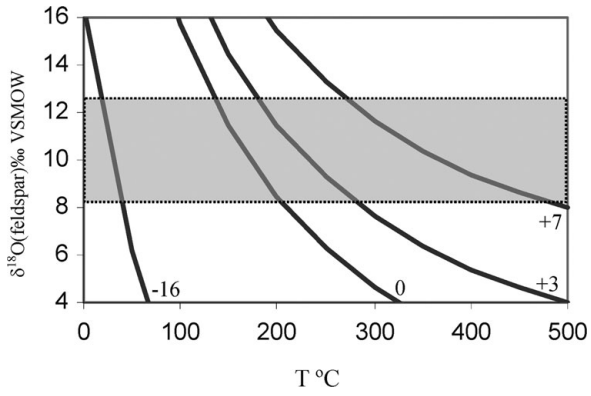

Figure 7. Material balance calculation of the variation of altered δ^{18}O(Afs) as a function of temperature and $\delta^{18}O(H_2O)$ during water–feldspar interaction. Calculated curves are for four different water compositions: +7 ‰ ('magmatic water'), +3 ‰ ('brine'), 0 ‰ (seawater) and −16 ‰ (average meteoric water at latitude 60°). Grey rectangle represents the field of measured δ^{18}O(Afs) in granitoids and associated rocks from southern Israel. The calculation assumes equilibrium exchange, initial δ^{18}O(Afs) of 7 ‰, and water/rock = ∞.

be explained by subsolidus closed-system oxygen exchange. Since Δ^{18}O(Qtz–Zrn) values are compatible with closed-system cooling in most plutons (except in the Timna porphyritic granite), the negative quartz-alkali feldspar fractionations imply a post-magmatic elevation of δ^{18}O(Afs) by an open-system exchange. The reaction occurred with an isotopically different oxygen reservoir, most probably hydrous fluids, and at a temperature below the exchange-by-diffusion closure temperature of quartz.

Large-scale interaction with heated meteoric water ($\delta^{18}O(H_2O) = -10$ to -20 ‰; ≥ 300 °C) has been shown to affect epizonal granitic plutons during emplacement and to profoundly alter their magmatic isotope ratios (Criss & Taylor, 1986). However, such high-temperature interactions would cause significant lowering of the δ^{18}O values of rocks and feldspar minerals and result in disequilibrium arrays below the expected closed-system fractionation line on the δ^{18}O(Afs)–δ^{18}O(Qtz) diagram (Fig. 6; Taylor, 1974; Criss & Taylor, 1983). In contrast, twelve quartz-alkali feldspar pairs from the southern Israel plutonic rocks form narrow elongated arrays above the 'closed system' fractionation line in Figure 6. This calls for different conditions for the water–rock interaction in southern Israel. With the purpose of constraining the temperature and $\delta^{18}O(H_2O)$ during alteration of feldspars in the study area, a material balance calculation for open-system conditions was conducted. To further maximize the effect of oxygen exchange on feldspar, the water/feldspar ratio is assumed to be infinite. The temperature dependence of the δ^{18}O value of alkali-feldspar that equilibrated with water of variable initial isotope ratio is presented in Figure 7. δ^{18}O(Afs)–T curves are shown for four representative initial δ^{18}O water compositions: present-day meteoric water at 60° latitude (−16 ‰), seawater (0 ‰), hypothetical 'sedimentary' water or brine (+3 ‰: Beyth *et al.* 1997) and magmatic water derived from an average alkaline-granite pluton (+7 ‰). Figure 7 demonstrates that the temperatures required to produce the observed range in δ^{18}O(Afs) by interaction with magmatic water expelled from the crystallizing pluton are 280–500 °C. However, interaction at such high temperatures would eventually also alter the isotope ratio of quartz (Clayton, Muffler & White, 1968). Since δ^{18}O(Qtz) has been shown above to reflect undisturbed cooling of the alkaline plutons, alteration by magmatic water is not possible. Likewise, alteration of feldspars during the Cambrian denudation, peneplanation and deep erosion of the northern Arabian–Nubian shield is highly unlikely. Isotope ratios of water involved in alteration and palaeosol formation on top of the exposed basement in southern Israel should resemble those of present-day meteoric water at 60° latitude (−16 ‰), the Early Cambrian palaeo-latitude of the area (Cocks & Torsvik, 2002). Such low-δ^{18}O water could produce the measured δ^{18}O(Afs) values at temperatures of 10 to 50 °C (Fig. 7). Raising the isotope ratio of feldspar by interaction at a very low temperature would have

required a prolonged process that eventually would have resulted in alteration of the feldspars to clays. Such a phenomenon is observed at the topmost several-metres-thick layer of the plutons, but cannot account for the wholesale alteration of feldspars at their present exposure levels. Thus, the alteration of feldspars in southern Israel plutons neither occurred during their Neoproterozoic emplacement nor during their Early Cambrian denudation and exposure. However, the material balance calculation allows alteration to occur with a variety of water types, including seawater (0 ‰) and water that have equilibrated with sedimentary rocks (+3 ‰) at a temperature range of 100–300 °C (Fig. 7).

Medium-temperature (~ 250 °C) interaction with high-δ^{18}O brines (+3 ‰) was suggested to account for the moderately negative Δ^{18}O(Qtz–Plg) = −1.4 ‰ and Δ^{18}O(Qtz–Afs) = −0.1 ‰ measured in the Timna porphyritic granite and Timna alkaline granite, respectively (Beyth *et al.* 1997). The hydrothermal activity presumably responsible for the ^{18}O/^{16}O-enrichments in the Timna igneous complex was attributed to circulation of brines through fractures related to the Dead Sea transform (Beyth *et al.* 1997; Matthews *et al.* 1999). The timing of the hydrothermal event was considered as Miocene, based on 'subrecent' remanent magnetic direction measured in the igneous rocks of Timna (Marco *et al.* 1993). None the less, a thermochronological study based on fission tracks in apatite demonstrated that the temperature in the Timna igneous rocks did not exceed 95 °C after the Cretaceous and 65 °C after Eocene times (Feinstein *et al.* 2003). Had fluids circulated through the Timna rocks at 250 °C during the Miocene, a fast and complete obliteration of apatite fission tracks should have occurred. Thus the secondary minerals, hematite and goethite, thought to induce the chemical remanent magnetization in the rocks of Timna (Marco *et al.* 1993), must have formed at $T \leq 65$ °C during the Miocene. Thermochronology shows, however, that a major thermal event occurred in southern Israel and Sinai in Early Carboniferous times (Kohn, Eyal & Feinstein, 1992). Temperatures as high as 225 ± 50 °C are indicated by total resetting of zircon fission track clocks and partial resetting of fission tracks in coexisting titanite crystals. Had hydrous fluids infiltrated the granites at such high thermal gradients, ^{18}O/^{16}O elevation in feldspar would have become inevitable.

7. Conclusions

(1) A-type granites in the Arabian–Nubian shield of southern Israel formed by variable processes simultaneously. In Timna, the alkaline granite evolved by differentiation of mantle-derived magma (Timna alkaline granite, δ^{18}O(Zrn) = 5.5 ‰), whereas significant supracrustal contribution is indicated by the Yehoshafat granite of the Elat area (δ^{18}O(Zrn) = 6.6 ‰).

(2) The igneous complex of Timna does not represent an exhumed static magma chamber. It evolved by fractional crystallization and possibly minor assimilation of alkaline mafic to intermediate magma at depth, followed by emplacement of plutons of variable composition and slightly variable δ^{18}O(Zrn) at shallow crustal levels.

(3) Diffusion modelling suggests that the initial cooling of the alkaline granite plutons down to 600 °C was very rapid (~ 1000 °C/Ma), probably due to very shallow emplacement. The host calc-alkaline granites of the post-collisional batholiths cooled at much a slower pace (~ 1–100 °C/Ma), indicating deeper emplacement. Decrease in emplacement depth of granites marks a fundamental change from thick orogenic to extended crust.

(4) Extensive water–rock interaction at ~ 100–250 °C significantly elevated the δ^{18}O values of feldspars. Thermochronology constrains the alteration event to the Early Carboniferous or earlier.

Acknowledgements. This study was supported by Israel Science Foundation grant no. 142/02. We thank M. Eyal, B. Litvinovsky and A. Zanvilevich for many helpful discussions. This paper greatly benefited from two anonymous reviews and constructive comments by editor D. Pyle.

References

AGRON, N. & BENTOR, Y. K. 1981. The volcanic massif of Biq'at Hayareah (Sinai–Negev), a case of potassium metasomatism. *Journal of Geology* **89**, 479–96.

BENTOR, Y. K. 1985. The crustal evolution of the Arabo-Nubian Massif with special reference to the Sinai Peninsula. *Precambrian Research* **28**, 1–74.

BEYTH, M., LONGSTAFFE, F. J., AYALON, A. & MATTHEWS, A. 1997. Epigenetic alteration of the Precambrian igneous complex at Mount Timna, southern Israel: Oxygen-isotope studies. *Israel Journal of Earth Sciences* **46**, 1–11.

BEYTH, M., STERN, R. J., ALTHERR, R. & KRÖNER, A. 1994. The Late Precambrian Timna igneous complex, southern Israel: Evidence for comagmatic-type sanukitoid monzodiorite and alkali granite magma. *Lithos* **31**, 103–24.

BLACK, R. & LIÉGEOIS, J. P. 1993. Cratons, mobile belts, alkaline rocks and continental lithospheric mantle: the Pan-African testimony. *Journal of the Geological Society, London* **150**, 89–98.

BONIN, B. 2007. A-type granites and relaed rocks: Evolution of a concept, problems and prospects. *Lithos* **97**, 1–29.

CLAYTON, R. N., GOLDSMITH, J. R. & MAYEDA, T. K. 1989. Oxygen isotope fractionation in quartz, albite, anorthite and calcite. *Geochimica et Cosmochimica Acta* **53**, 725–33.

CLAYTON, R. N., MUFFLER, L. J. P. & WHITE, D. E. 1968. Oxygen isotope study of calcite and silicates of the River Ranch No. 1 well, Salton sea geothermal field, California. *American Journal of Science* **266**, 968–79.

COCKS, L. R. M. & TORSVIK, T. H. 2002. Earth geography from 500 to 400 million years ago: a faunal and palaeomagnetic review. *Journal of the Geological Society, London* **159**, 631–44.

COLLINS, W. J., BEAMS, S. D., WHITE, A. J. R. & CHAPPELL, B. W. 1982. Nature and origin of A-type granites

with particular reference to Southeastern Australia. *Contributions to Mineralogy and Petrology* **80**, 189–200.

CREASER, R. A., PRINCE, R. C. & WORMAN, R. J. 1991. A-type granites revisited: assessment of a residual-source model. *Geology* **19**, 163–6.

CRISS, R. E. & TAYLOR, H. P. JR. 1983. An $^{18}O/^{16}O$ and D/H study of tertiary hydrothermal systems in the southern half of the Idaho batholith. *Geological Society of America Bulletin* **94**, 640–63.

CRISS, R. E. & TAYLOR, H. P. JR. 1986. Meteoric-hydrothermal systems. In *Stable isotopes in high temperature geological processes* (eds J. W. Valley, H. P. Taylor Jr & J. R. O'Neil), pp. 373–424. Washington, DC: Mineralogical Society of America. *Reviews in Mineralogy* **16**.

EBY, G. N. 1990. The A-type granitoids: a review of their occurrence and chemical characteristics and speculations on their petrogenesis. *Lithos* **26**, 115–34.

EBY, G. N. 1992. Chemical subdivision of the A-type granitoids: petrogenetic and tectonic implications. *Geology* **20**, 641–4.

EILER, J. M., BAUMGARTNER, L. P. & VALLEY, J. W. 1992. Intercrystalline stable isotope diffusion: a fast grain boundary model. *Contributions to Mineralogy and Petrology* **112**, 543–57.

EILER, J. M., BAUMGARTNER, L. P. & VALLEY, J. W. 1994. Fast grain boundary: A FORTRAN-77 program for calculating the effects of retrograde interdiffusion of stable isotopes. *Computers & Geosciences* **20**, 1415–34.

EYAL, M. & HEZKIYAHU, T. 1980. Katherina Pluton: the outline of a petrologic framework. *Israel Journal of Earth Sciences* **29**, 41–52.

EYAL, M., LITVINOVSKY, B. A., KATZIR, Y. & ZANVILEVICH, A. N. 2004. The Pan-African high K calc-alkaline peraluminous Elat Granite from southern Israel: geology, geochemistry and petrogenesis. *Journal of African Earth Sciences* **40**, 115–36.

EYAL, M. & PELTZ, S. 1994. The structure of the Ramat Yotam caldera, southern Israel: a deeply eroded Late Precambrian ash-flow caldera. *Israel Journal of Earth Sciences* **43**, 81–90.

FEINSTEIN, S., EYAL, M., STECKLER, M. S., KOHN, B. P., IBRAHIM, K. & MOH'D, B. K. 2003. Phanerozoic thermo-tectonic history of the Northern margin of the Arabo-Nubian shield across the Dead Sea transform. *BSF Grant Report No. **97-248***, 45–57.

FROST, B. R., BARNES, C. G., COLLINS, W. J., ARCULUS, R. J., ELLIS, D. J. & FROST, C. D. 2001. A geochemical classification for granitic rocks. *Journal of Petrology* **42**, 2033–48.

FURNES, H., EL-SAYED, M. M., KHALIL, S. O. & HASSANEN, M. A. 1996. Pan-African magmatism in the Wadi El-Imra district, Central Eastern Desert, Egypt: geochemistry and tectonic environment. *Journal of the Geological Society, London* **153**, 705–18.

GARFUNKEL, Z. 1980. Contribution to the geology of the Precambrian of the Elat area. *Israel Journal of Earth Sciences* **29**, 25–40.

GARFUNKEL, Z. 1999. History and paleogeography during the Pan-African orogen to stable platform transition: Reappraisal of the evidence from the Elat area and the Northern Arabian–Nubian Shield. *Israel Journal of Earth Sciences* **48**, 135–57.

GENNA, A., NEHLIG, P., LE GOFF, E., GUERROT, C. & SHANTI, M. 2002. Proterozoic tectonism of the Arabian Shield. *Precambrian Research* **117**, 21–40.

HANCHAR, J. M. & WATSON, E. B. 2003. Zircon saturation thermometry. In *Zircon* (eds J. M. Hanchar & P. W. O. Hoskin), pp. 89–112. *Reviews in Mineralogy and Geochemistry* **53**. Washington DC: Mineralogical Society of America.

HANSMANN, W. & OBERLI, F. 1991. Zircon inheritance in an igneous rock suite from the Southern Adamello batholith (Italian Alps). *Contribution to Mineralogy and Petrology* **107**, 501–18.

JARRAR, G., STERN, R. J., SAFFARINI, G. & AL-ZUBI, H. 2003. Late and post-orogenic Neoproterozoic intrusions of Jordan: implications for crustal growth in the northernmost segment of the East African Orogen. *Precambrian Research* **123**, 295–319.

JOHNSON, P. R. & WOLDEHAIMANOT, B. 2003. Development of the Arabian–Nubian Shield; perspectives on accretion and deformation in the Northern East African Orogen and the assembly of Gondwana. In *Proterozoic East Gondwana; supercontinent assembly and breakup* (eds M. Yoshida, B. F. Windley & S. Dasgupta), pp. 289–325. Geological Society of London, Special Publication no. 206.

KATZ, O., AVIGAD, D., MATTHEWS, A. & HEIMANN, A. 1998. Precambrian metamorphic evolution of the Arabian–Nubian Shield in the Roded area, southern Israel. *Israel Journal of Earth Sciences* **47**, 93–110.

KATZIR, Y., EYAL, M., LITVINOVSKY, B. A., JAHN, B. M., ZANVILEVICH, A. N., VALLEY, J. W., BEERI, Y., PELEI, I. & SHIMSHILASHVILI, E. 2007*a*. Petrogenesis of A-type granites and origin of vertical zoning in the Katharina pluton, area of Gebel Mussa (Mt. Moses), Sinai, Egypt. *Lithos* **95**, 208–28.

KATZIR, Y., LITVINOVSKY, B., EYAL, M., ZANVILEVICH, A. N. & VAPNIK, YE. 2006. Four successive episodes of Late Pan-African dikes in the central Elat area, southern Israel. *Israel Journal of Earth Sciences* **55**, 69–93.

KATZIR, Y., LITVINOVSKY, B., JAHN, B. M., EYAL, M., ZANVILEVICH, A. N., VALLEY, J. W., VAPNIK, YE., BEERI, Y. & SPICUZZA, M. J. 2007*b*. Interrelations between coeval mafic and A-type silicic magmas from composite dykes in a bimodal suite of southern Israel, Northernmost Arabian–Nubian Shield: Geochemical and isotope constraints. *Lithos* **97**, 336–64.

KESSEL, R., STEIN, M. & NAVON, O. 1998. Petrogenesis of Late Neoproterozoic dikes in the Northern Arabian–Nubian Shield: implications for the origin of A-type granites. *Precambrian Research* **92**, 195–213.

KING, E. M. & VALLEY, J. W. 2001. Oxygen isotope study of magmatic source, assimilation and alteration in the Idaho batholith. *Contributions to Mineralogy and Petrology* **142**, 72–88.

KING, E. M., VALLEY, J. W., DAVIS, D. W. & EDWARDS, G. R. 1998. Oxygen isotope ratios of Archean plutonic zircons from granite–greenstone belts of the Superior Province: indicator of magmatic source. *Precambrian Research* **92**, 365–87.

KING, E. M., VALLEY, J. W., DAVIS, D. W. & KOWALLIS, B. J. 2001. Empirical determination of oxygen isotope fractionation factors for titanite with respect to zircon and quartz. *Geochimica et Cosmochimica Acta* **65**, 3165–75.

KOHN, B. P., EYAL, M. & FEINSTEIN, S. 1992. A major Late Devonian–Early Carboniferous thermotectonic event at the NW margin of the Arabian–Nubian Shield: evidence from zircon fission track dating. *Tectonics* **11**, 1018–27.

KOHN, M. J. & VALLEY, J. W. 1998. Oxygen isotope geochemistry of the amphiboles: isotope effects of cation

substitutions in minerals. *Geochimica et Cosmochimica Acta* **62**, 1947–58.

KRÖNER, A., EYAL, M. & EYAL, Y. 1990. Early Pan-African evolution of the basement around Elat, Israel, and the Sinai Peninsula revealed by single-zircon evaporation dating, and implications for crustal accretion rates. *Geology* **18**, 545–8.

LOISELLE, M. C. & WONES, D. R. 1979. Characteristics and origin of anorogenic granites. *Geological Society of America, Abstracts and Program* **11**, 468.

MARCO, S., RON, H., MATTHEWS, A., BEYTH, M. & NAVON, O. 1993. Chemical remanent magnetism related to the Dead Sea rift: Evidence from Precambrian igneous rocks of Timna, southern Israel. *Journal of Geophysical Research* **98**, 16001–12.

MATTEY, D. P., LOWRY, D. & MACPHERSON, C. G. 1994. Oxygen isotope composition of the mantle. *Earth and Planetary Science Letters* **128**, 231–41.

MATTEY, D. P., LOWRY, D., MACPHERSON, C. G. & CHAZOT, G. 1994. Oxygen isotope composition of mantle minerals by laser fluorination analysis: homogeneity in peridotites, heterogeneity in eclogites. *Mineralogical Magazine* **58**, 573–4.

MATTHEWS, A., AYALON, A., ZIV, A. & SHAKED, J. 1999. Hydrogen and oxygen isotope studies of alteration in the Timna igneous complex. *Israel Journal of Earth Sciences* **48**, 121–31.

MEERT, J. G. 2003. A synopsis of events related to the assembly of eastern Gondwana. *Tectonophysics* **362**, 1–40.

MUSHKIN, A., NAVON, O., HALICZ, L., HARTMANN, G. & STEIN, M. 2003. The petrogenesis of A-type magmas from the Amram Massif, southern Israel. *Journal of Petrology* **44**, 815–32.

MUSHKIN, A., NAVON, O., HALICZ, L., HEIMANN, A., WOERNER, G. & STEIN, M. 1999. Geology and geochronology of the Amram Massif, Southern Negev desert, Israel. *Israel Journal of Earth Sciences* **48**, 179–93.

PAGE, F. Z., USHIKUBO, T., KITA, N. T., RICIPUTI, L. R. & VALLEY, J. W. 2007. High-precision oxygen isotope analysis of picogram samples reveals 2 µm gradients and slow diffusion in zircon. *American Mineralogist* **92**, 1772–5.

PECK, W. H., KING, E. M. & VALLEY, J. W. 2000. Oxygen isotope perspective on Precambrian crustal growth and maturation. *Geology* **28**, 363–6.

POLLACK, H. M. 1986. Cratonization and thermal evolution of the mantle. *Earth and Planetary Science Letters* **80**, 175–82.

SEGEV, A., GOLDSHMIDT, V. & RYBAKOV, M. 1999. Late Precambrian–Cambrian tectonic setting of the crystalline basement in the northern Arabian–Nubian Shield as derived from gravity and magnetic data: Basin-and-range characteristics. *Israel Journal of Earth Sciences* **48**, 159–78.

SHPITZER, M., BEYTH, M. & MATTHEWS, A. 1992. Igneous differentiation in the Late Precambrian plutonic rocks of Mt. Timna. *Israel Journal of Earth Sciences* **40**, 17–27.

SPICUZZA, M. J., VALLEY, J. W, KOHN, M. J., GIRARD, J. P. & FOUILLAC, A. M. 1998. The rapid heating, defocused beam technique: a CO_2-laser-based method for highly precise and accurate determination of $\delta^{18}O$ values of quartz. *Chemical Geology* **144**, 195–203.

SPICUZZA, M. J., VALLEY, J. W. & MCCONNELL, V. S. 1998. Oxygen isotope analysis of whole rock via laser fluorination: an air-lock approach. *Geological Society of America, Annual Meeting, Abstracts with Program* **30**, 80.

STEIN, M. 2003. Tracing the plume material in the Arabian–Nubian Shield. *Precambrian Research* **123**, 223–34.

STEIN, M. & GOLDSTEIN, S. L. 1996. From plume head to continental lithosphere in the Arabian–Nubian shield. *Nature* **382**, 773–8.

STEIN, M. & HOFFMANN, A. W. 1992. Fossil plume head beneath the Arabian Lithosphere? *Earth and Planetary Science Letters* **114**, 193–203.

STERN, R. J. 1994. Arc assembly and continental collision in the Neoproterozoic East African orogen. Implications for the consolidation of Gondwanaland. *Annual Review of Earth and Planet Sciences* **22**, 319–51.

STERN, R. J. 2002. Crustal evolution in the East African Orogen: a neodymium isotopic perspective. *Journal of African Earth Sciences* **34**, 109–17.

STERN, R. J. & ABDELSALAM, M. G. 1998. Formation of continental crust in the Arabian–Nubian Shield: evidence from granitic rocks of the Nakasib suture, NE Sudan. *Geologische Rundschau* **87**, 150–60.

STERN, R. J. & GOTTFRIED, D. 1986. Petrogenesis of the Late Precambrian (575–600 Ma) bimodal suite in northeast Africa. *Contributions to Mineralogy and Petrology* **24**, 492–501.

STERN, R. J. & KRÖNER, A. 1993. Late Precambrian crustal evolution in NE Sudan, isotopic and geochronologic constraints. *Journal of Geology* **101**, 555–74.

STERN, R. J., SELLERS, G. & GOTTFRIED, D. 1988. Bimodal dike swarms in the north of the Eastern Desert of Egypt: Significance for the origin of the Precambrian "A-type" Granites in Northern Afro-Arabia. In *The Pan-African Belt of NE Africa and Adjacent Areas: Tectonic Evolution and Economic Aspects* (eds R. Greiling & R. Gaby), pp. 147–79. Braunschweig, Germany: Frieder, Vieweg and Sohn.

STOESER, D. B. & CAMP, V. E. 1985. Pan-African microplate accretion of the Arabian shield. *Geological Society of America Bulletin* **96**, 817–26.

TAYLOR, H. P. JR. 1974. The application of oxygen and hydrogen isotope studies to problems of hydrothermal alteration and ore deposition. *Economic Geology* **69**, 843–83.

TURNER, S. P., FODEN, J. D. & MORRISON, R. S. 1992. Derivation of some A-type magmas by fractionation of basaltic magma: an example from the Padthaway Ridge, south Australia. *Lithos* **28**, 151–79.

VALLEY, J. W. 2001. Stable isotope thermometry at high temperatures. In *Stable Isotope Geochemistry* (eds J. W. Valley & D. R. Cole), pp. 365–91. *Reviews in Mineralogy and Geochemistry* **43**. Washington DC: Mineralogical Society of America.

VALLEY, J. W. 2003. Oxygen isotopes in zircon. In *Zircon* (eds J. M. Hanchar & P. W. O. Hoskin), pp. 343–86. *Reviews in Mineralogy and Geochemistry* **53**. Washington DC: Mineralogical Society of America.

VALLEY, J. W., BINDEMAN, I. N. & PECK, W. H. 2003. Empirical calibration of oxygen isotope fractionation in zircon. *Geochimica et Cosmochimica Acta* **67**, 3257–66.

VALLEY, J. W., CHIARENZELLI, J. R. & MCLELLAND, J. M. 1994. Oxygen isotope geochemistry of zircon. *Earth and Planetary Science Letters* **126**, 187–206.

VALLEY, J. W., KINNY, P. D., SCHULZE, D. J. & SPICUZZA, M. J. 1998. Zircon megacrysts from kimberlite: oxygen isotope variability among mantle melts. *Contributions to Mineralogy and Petrology* **133**, 1–11.

VALLEY, J. W., KITCHEN, N., KOHN, M. J., NIENDORF, C. R. & SPICUZZA, M. J. 1995. UWG-2, a garnet

standard for oxygen isotope ratios: Strategies for high precision and accuracy with laser heating. *Geochimica et Cosmochimica Acta* **59**, 5523–31.

VALLEY, J. W., LACKEY, J. S., CAVOSIE, A. J., CLECHENKO, C. C., SPICUZZA, M. J., BASEI, M. A. S., BINDEMAN, I. N., FERREIRA, V. P., SIAL, A. N., KING, E. M., PECK, W. H., SINHA, A. K. & WEI, C. S. 2005. 4.4 billion years of crustal maturation: oxygen isotope ratios of magmatic zircon. *Contribution to Mineralogy and Petrology* **150**, 561–80.

VON BLANKENBURG, F. 1992. Combined high-precision chronometry and geochemical tracing using accretionary minerals: applied to the Central-Alpine Bergel intrusion (central Europe). *Chemical Geology* **100**, 19–40.

WATSON, E. B. & HARRISON, T. M. 1983. Zircon saturation revisited: temperature and composition effects in a variety of crustal magma types. *Earth and Planetary Science Letters* **64**, 295–304.

WHALEN, J. B., CURRIE, K. L. & CHAPPELL, B. W. 1987. A-type granites: Geochemical characteristics, discrimination and petrogenesis. *Contributions to Mineralogy and Petrology* **95**, 407–19.

WHALEN, J. B., JENNER, G. A., CURRIE, K. L., BARR, S. M., LONGSTAFFE, F. J. & HEGNER, E. 1994. Geochemical and isotopic characteristics of granitoids of the Avalon Zone, Southern New Brunswick: possible evidence for repeated delamination events. *Geology* **102**, 269–72.

WHALEN, J. B., JENNER, G. A., LONGSTAFFE, F. J., ROBERT, F. & GARIEPY, C. 1996. Geochemical and isotopic (O, Nd, Pb and Sr) constraints on A-type granite petrogenesis based on the Topsails igneous suite, Newfoundland Appalachians. *Journal of Petrology* **37**, 1463–89.

WINDLEY, B. F. 1993. Proterozoic anorogenic magmatism and its orogenic connections. *Journal of the Geological Society, London* **150**, 39–50.